13th Australasian Fluid Mechanics Conference
Monash University, Melbourne, Australia
13-18 December 1998

SUPERCRITICAL AND SUBCRITICAL LONG'S VORTICES

Ramón FERNÁNDEZ-FERIA

E. T. S. Ingenieros Industriales
Universidad de Málaga, 29013 Malaga, SPAIN

ABSTRACT

A spatial linear stability analysis of Long's vortex shows that, although both Type I and Type II vortices are convectively unstable for counter-rotating spiral modes, only Type II Long's vortices with negative axial velocity at the axis can in addition sustain unstable spiral modes with negative group velocities. Thus, Type I and Type II Long's vortices are supercritical and subcritical swirling flows in Benjamin's sense, respectively, the transition between the two types of flows taking place when the axial velocity at the axis becomes zero.

INTRODUCTION

Long's (1961) vortex has been extensively considered as a simple model for high Reynolds number vortices of geophysical and engineering interest, mainly because it is an exact solution to the near-axis approximation of the Navier-Stokes equation which is non-parallel and consistently includes a relatively important axial flow, both characteristics present in most real vortices of interest. In particular, its stability has been analysed by a number of authors using different techniques and degrees of approximation, with the main objective of trying to elucidate and predict some of the interesting properties that highly swirling flows present in practice. Most of these previous works considered the *temporal* stability (i.e. with given real wave number and unknown complex frequency) of Long's vortex using a parallel flow approximation (see, e.g., Fernández-Feria (1996) for the most significant references; in that work, hereafter referred to as T, the effect of viscosity and of the non-parallelism of the basic flow is also taken into account in the temporal stability analysis of Long's vortex). In the present work, the results of a *spatial* stability analysis (i.e. with given real frequency look for the complex axial wave number) of Long's vortex which also takes into account the effect of viscosity and the non-parallelism of the basic flow (locally) are reported. The spatial analysis is more appropriate to study the evolution of waves as they propagate from a given forced oscillation at a given location, which is the situation usually met in experiments. It is shown that the local spatial analysis reproduces the results of the temporal instability calculations when the group velocity is positive (convective instabilities). However, new unstable counter-rotating spiral modes with negative group velocities are found here using the spatial formulation for Type II vortices, not found with the temporal analysis. As discussed in the last section, these new unstable modes establish a fundamental difference between Type I and Type II Long's vortices.

FORMULATION OF THE PROBLEM

The basic vortex.

Long's vortex is a similarity solution to the near-axis boundary layer approximation of the steady, incompressible and axisymmetric Navier-Stokes equations, matching an inviscid flow with velocity and pressure fields inversely proportional to the distance r to the axis of symmetry. Long (1961) showed that there are two solutions for $M > M^*$ (termed as Type I and Type II solutions by Burggraf and Foster (1977)), and none for $M < M^*$, where M is the dimensionless flow force and $M^* \simeq 3.75$ is a critical value. In cylindrical polar co-ordinates (r, θ, z), the vortex has the self-similar structure

$$\Psi = \nu z f(\xi) \quad , \tag{1}$$

$$V = \frac{\nu z}{\delta^2(z)}\gamma(\xi) \quad , \quad \frac{P}{\rho} = \frac{(\nu z)^2}{\delta^4(z)}\beta(\xi) \quad , \tag{2}$$

where Ψ is the stream function for the meridional motion, through which the axial and radial velocity components, W and U, are:

$$W = \frac{\nu z}{\delta^2} 2f'(\xi), \; U = -\frac{\nu}{r}[f(\xi) - 2\xi f'(\xi)] \; ; \tag{3}$$

V is the azimuthal velocity component, ν the kinematic viscosity, and $\delta(z)$ the vortex core thickness,

$$\delta(z) = \frac{\nu z}{W_o} \quad , \tag{4}$$

W_o being a constant with the same dimensions as ν characterizing the external inviscid flow; the similarity variable ξ is defined by

$$\xi \equiv \eta^2 \quad , \quad \eta = \frac{r}{\delta(z)} \quad . \tag{5}$$

The functions f, γ and β are governed by a set of three non-linear ordinary differential equations (see T). An unique solution exists for each value of the non-dimensional axial velocity at the axis, $A_1 \equiv f'(0)$, in the allowed interval $-1/\sqrt{2} < A_1 < \infty$. Type I solutions have a positive axial velocity at the axis, with A_1 within the interval (A_1^*, ∞), where $A_1^* \simeq 0.15$ corresponds to the critical (or folding) value of M, while most Type II solutions have a negative axial velocity at the axis, with A_1 in the interval $(-1/\sqrt{2}, A_1^*)$(see Fig. 1). In the limit of large A_1 (M large), Type I solution corresponds to an intense swirling jet with large positive axial velocity at the axis, while for $A_1 \to -1/\sqrt{2}$ (again M large), Type II solution has the form of a ring-jet with large positive axial flow on the ring and negative axial flow in its interior (see Foster and Smith (1989) for asymptotic solutions in these two limits).

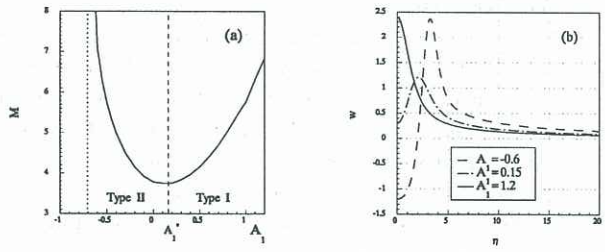

Figure 1: **(a)** Function $M(A_1)$. **(b)** Axial velocity profiles for three different values of A_1.

Stability formulation and numerical method.

The flow variables, (u, v, w) and p, are decomposed, as usual, into a mean part, (U, V, W) and P, and a small perturbation. After (2)-(3),

$$w = \frac{\nu z}{\delta^2}[2f' + \overline{w}] \quad , \quad u = \frac{\nu}{r}[-f + 2\xi f' + \frac{rz}{\delta^2}\overline{u}] \quad , \tag{6}$$

$$v = \frac{\nu z}{\delta^2}[\gamma + \overline{v}] \quad , \quad \frac{p}{\rho} = \frac{(\nu z)^2}{\delta^4}[\beta + \overline{p}] \, , \tag{7}$$

where the perturbations are written in the standard form

$$\mathbf{s} \equiv [\overline{u}, \overline{v}, \overline{w}, \overline{p}]^T \equiv \mathbf{S}(x, \xi)\chi(x, \theta, t), \; x \equiv \frac{z}{z_o}, \tag{8}$$

with the complex amplitude,

$$\mathbf{S}(x, \xi) = [iF(x, \xi), G(x, \xi), H(x, \xi), \Pi(x, \xi)]^T, \tag{9}$$

and the exponential part describing the wave-like nature of the disturbances,

$$\chi(x, \theta, t) = \exp\left[\frac{1}{\Delta_o}\int_{x_o}^{x} a(x')dx' + i(n\theta - \Omega t)\right]. \tag{10}$$

The use of an axial scale-length z_o in addition to the radial characteristic length δ_o, defined as the vortex thickness at z_o, $\delta_o = \nu z_o / W_o$, allows the definition of the non-dimensional parameter $\Delta_o \equiv \frac{\delta_o}{z_o} = \frac{\nu}{W_o}$, which is assumed to be small within the present near-axis boundary layer approximation (note that terms $O(\Delta_o^2)$ are neglected in the derivation of Long's vortex). The non-dimensional, order of unity, axial wavenumber a is defined as δ_o times the dimensional wave number k:

$$a(x) \equiv \delta_o k(x) \equiv \gamma(x) + i\alpha(x) \, , \tag{11}$$

which accounts for the fast, wave-like variation of the perturbations. Its real part $\gamma(x)$ is the exponential growth rate, and the imaginary part $\alpha(x)$ is the axial wavenumber. A non-dimensional, order of unity, frequency ω is also defined:

$$\omega = \frac{\Omega \delta_o^3}{\nu z_o}. \tag{12}$$

Substituting (6)-(12) into the incompressible Navier-Stokes equations, and neglecting second-order terms in both the small perturbations and the inverse of the local Reynolds number,

$$Re^{-1} \equiv \Delta(z) \equiv \frac{\delta(z)}{z} = \Delta_o \ll 1, \tag{13}$$

(note that the local Reynolds number is constant along the axis in Long's vortex), a set of linear *parabolized* stability equations results for $\mathbf{S}$, a and ω. In these equations, the small terms $O(\Delta)$ take into account three different effects on the stability of the perturbations: the effect of viscosity, the effect of the non-parallelism of the basic flow, and the effect of the streamwise evolution of the perturbations. Here, as in T, this last effect will be neglected, so that the terms proportional to the streamwise derivatives $\partial \mathbf{S}/\partial x$ will disappear from the equations, thus becoming a set of ordinary differential equations instead of partial differential equations (it is shown elsewhere that these terms accounting for the history of the perturbations are relatively important only for low Reynolds numbers when the growth rate is very small). The resulting *local* stability equations, which include the effect of viscosity and the non-parallelism of the flow partially, may be written as:

$$[L_{oo} + \Delta L_{o1} + aL_1 + a^2 \Delta L_2]\mathbf{S} = 0, \tag{14}$$

where L_{oo}, L_{o1}, L_1 and L_2 are linear, order of unity, operators which depend on x and ξ (note that only the operators L_{oo} and L_1 would appear in an inviscid stability analysis with parallel flow approximation). L_{oo} depends linearly on the frequency ω and contains $\partial/\partial\xi$ terms, while L_{o1} contains both $\partial/\partial\xi$ and $\partial^2/\partial\xi^2$ terms. This equation is solved with the following homogeneous radial boundary conditions:

$$\xi \to \infty : \quad F = G = H = 0; \tag{15}$$

$$\xi = 0 : \quad F = G = 0, \partial H/\partial\xi = 0, (n = 0), \tag{16}$$

$$F \pm G = 0, \partial F/\partial\xi = 0, H = 0, (n = \pm 1), \tag{17}$$

$$F = G = H = 0, \quad (|n| > 1). \tag{18}$$

For the spatial stability analysis considered here, (14)-(18) constitute a non-linear eigenvalue problem where, given a real frequency ω, one looks for the complex eigenvalues a and complex eigenfunctions $\mathbf{S}$. For a given basic vortex (A_1), azimuthal wave number (n), and axial location (x), the flow is unstable for the chosen frequency if the real part of a, γ, is positive. To solve numerically the problem, the $\xi-$dependence of $\mathbf{S}$ is discretized using a staggered Chebyshev spectral collocation technique developed by Khorrami (1991). This method has the advantage of eliminating the need of two artificial pressure boundary conditions at $\xi = 0$ and $\xi = \infty$, which for that reason are not included in (15)-(18). The boundary conditions at infinity (15) are applied at a truncated radial distance ξ_{max}, chosen large enough to ensure that the results do not depend on that truncated distance ($\xi_{max} = 5000$ was used in most of the reported computations). A non-uniform co-ordinate transformation is used to map the interval $0 \le \xi \le \xi_{max}$ into the Chebishev polynomials domain $-1 \le s \le 1$, $\xi = c_1(1+s)/(c_2 - s)$, where c_1 is a constant ($c_1 = 3$ in all the computations) and $c_2 = 1 + 2c_1/\xi_{max}$. This transformation allows large values of ξ to be taken into account with relatively few basis functions. The $\xi-$domain is thus discretized in N points, N being the number of Chebyshev polynomials in which $\mathbf{S} = [iF, G, H, \Pi]^T$ has been expanded. In the results presented here, N ranged between 40 and 100. Once discretized, the non-linear eigenvalue problem is solved using the linear companion matrix method described by Bridges and Morris (1984). The resulting (complex) linear eigenvalue problem of dimension $8N$ is solved with the IMSL subroutine DGVCCG, which provides the entire eigenvalue and eigenvector spectrum. Owing to the fact that the matrices to solve the spatial eigenvalue problem are twice as larger than the matrices in the temporal eigenvalue problem for the same value of N, the computation time is about eight times larger. Also, due to the large dimensions of the matrices in (14), a relatively large amount of spurious numerical eigenvalues with very small wavenumbers (large wavelengths) are produced by the eigenvalue solver, particularly when ω is also very small. They are easily discarded, however, because the corresponding growth rates γ increase without bound with N, instead of rapidly converging to a given finite value as it happens for eigenvalues corresponding to physical modes. Thus, a minimum or cut-off value of α has to be used when looking for the most unstable mode (highest γ) for a given frequency and flow parameters. This lower limit is easily selected by just increasing N.

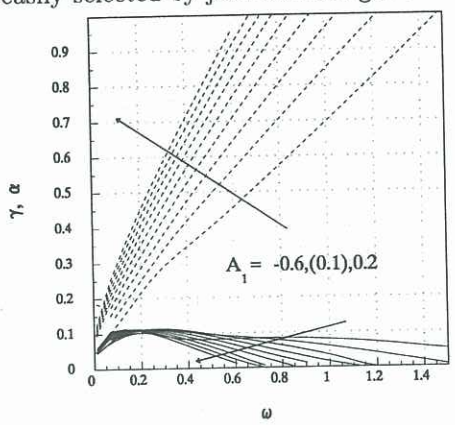

Figure 2: $\gamma(\omega)$ (continuous lines) and $\alpha(\omega)$ (dashed lines) for convectively unstable modes with $n = -1$, for $x = 1$, $\Delta_o = 0.001$ and increasing values of A_1. $N = 40$ and 60.

RESULTS AND DISCUSSION

Figure 2 shows the growth rates (γ) and axial wavenumbers (α) of the most unstable inviscid ($\Delta = 10^{-3}$) modes with positive group velocities ($c_g \equiv \partial\omega/\partial\alpha > 0$) for azimuthal wavenumber $n = -1$ and values of A_1 ranging from 0.2 (Type I vortex near the folding value A_1^*) to -0.6 (Type II vortex near its minimum value $-1/\sqrt{2}$). The maximum growth rate is always about 0.1, with the range of unstable frequencies increasing as A_1 decreases. These *convectively* unstable modes are the most unstable ones for $A_1 > 0$, and correspond to those obtained with the temporal stability analysis of T. However, as shown in Fig. 3, the spatial analysis reveals the existence of highly unstable modes with negative group velocities for $A_1 < 0$, which do not exist for $A_1 > 0$. In fact, $c_g \to 0$ as $A_1 \to 0^-$ (see Fig. 4). For $-A_1$ small, both the growth rate and the wavenumber are very large for low frequencies, with $c_g(\omega)$ almost constant for all values of ω. As A_1 decreases, γ decreases, but remaining always larger than the corresponding to the convectively unstable modes of Fig. 2, and $-c_g$ increases.

For A_1 very near its minimum value $-1/\sqrt{2}$, a bunch of unstable modes, both with positive and negative c_g, appears. The unstable mode for $A_1 = -0.7$ plotted in Fig.3 does not correspond to that with largest γ, which has $c_g > 0$ and it is neither plotted in Fig.2, but to the one with $c_g < 0$ in some frequency range (note that $c_g \to -\infty$ for $\omega \approx 0.2$).

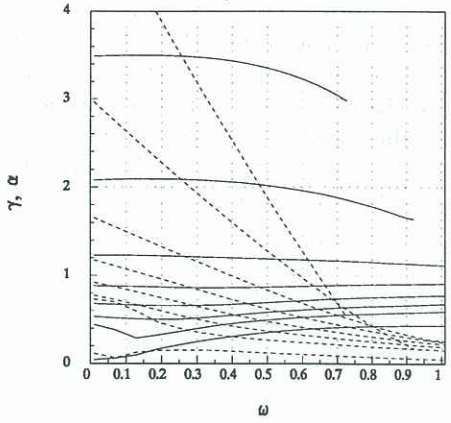

Figure 3: $\gamma(\omega)$ (continuous lines) and $\alpha(\omega)$ (dashed lines) for modes with $n = -1$ and $c_g < 0$. $x = 1$, $\Delta_o = 0.001$ and $A_1 = 0.05, 0.1, (0.1), -0.7$ (top to bottom). $N = 100$.

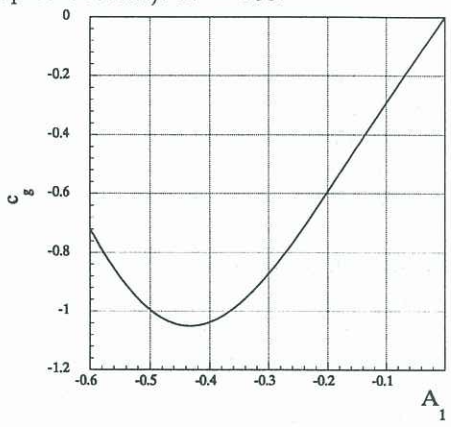

Figure 4: Group velocity at $\omega = 0.2$ for the unstable modes of Fig. 3.

These results show that Type II Long's vortices with $A_1 < 0$ can sustain both upstream- and downstream-propagating unstable modes with $n = -1$, so that they are subcritical in Benjamin's (1962) sense. Type I Long's vortices, on the other hand, are supercritical because they can only sustain downstream-propagating, or convective, unstable modes. This fundamental difference between Type I and Type II Long's vortices has to be added to that found in T, where it was shown that only Type II Long's vortices are unstable for axisymmetric ($n = 0$) disturbances. Another interesting result is that, although convectively unstable modes for Type II flows exist for any value of the azimuthal wave number n, unstable modes with $c_g < 0$ exist *only* for counter-rotating spiral modes *with* $n = -1$: As shown in Fig. 5 for $A_1 = -0.5$, the most unstable mode with $n = -2$ has $c_g > 0$, as it occurs for co-rotating spiral disturbances and for axisymmetric disturbances ($n = +1$ and $n = 0$ in Fig. 5; note that the growth rate for axisymmetric disturbances is about an order of magnitude smaller than for non-axisymmetric ones).

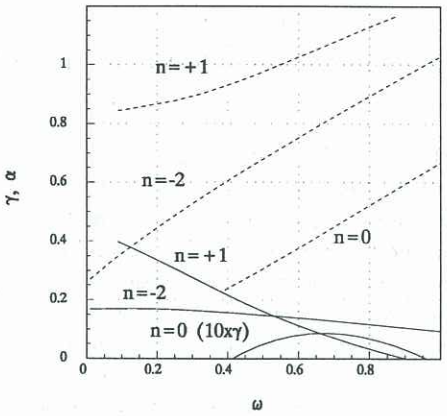

Figure 5: $\gamma(\omega)$ (continuous lines) and $\alpha(\omega)$ (dashed lines) for the most unstable modes when $A_1 = -0.5$ for $x = 1$, $\Delta_o = 0.001$ and $n = 0, +1, -2$. $N = 100$.

REFERENCES

BENJAMIN, T.B., "Theory of vortex breakdown phenomenon", *J. Fluid Mech.*, **14,** 529-551, 1962.

BRIDGES, T.J. and MORRIS, P.J., "Differential eigenvalue problems in which the parameter appears nonlinearly", *J. Comput. Phys.*, **55,** 437-460, 1984.

BURGGRAF, O.R. and FOSTER, M.R., "Continuation and breakdown in tornado-like vortices", *J. Fluid Mech.*, **80,** 685-703, 1977.

FERNÁNDEZ-FERIA, R., "Viscous and inviscid instabilities of non-parallel self-similar axisymmetric vortex cores", *J. Fluid Mech.*, **323,** 339-365, 1996.

FOSTER, M.R. and SMITH, F.T., "Stability of Long's vortex at large flow force", *J. Fluid Mech.*, **206,** 405-432, 1989.

KHORRAMI, M.R., "A Chebyshev spectral collocation method using a staggered grid for the stability of cylindrical flows", *Int. J. Num. Methods Fluids,* **12,** 825-833, 1991.

LONG, R.L., "A vortex in an infinite fluid", *J. Fluid Mech.*, **11,** 611-625, 1961.